A98-31540 ICAS-98-3,3,2

QUANTITATIVE AND QUALITATIVE ASPECTS OF THE SHEAR-SENSITIVE LIQUID CRYSTAL COATING METHOD

Daniel C. Reda and Michael C. Wilder

Fluid Mechanics Laboratory (MS:260-1)
NASA-Ames Research Center
Moffett Field, CA 94035-1000

Abstract

When a shear-sensitive liquid crystal coating is applied to a planar surface and illuminated from the normal direction by white light, then observed from an oblique above-plane view angle, its color-change response to shear depends on both shear stress vector magnitude and the direction of the applied shear vector relative to the observer's in-plane line of sight. At any surface point, the maximum color change is always seen or measured when the local shear vector is aligned with, and directed away from, the observer; the magnitude of the color change at this vector/observer aligned orientation scales directly with shear stress magnitude. Conversely, any surface point exposed to a shear vector with a component directed toward the observer exhibits a non-color-change response, always characterized by a rusty red or brown color, independent of both shear magnitude and shear direction. Surface slope inclinations of ±15 deg, measured relative to the planar-surface baseline, have been shown not to alter these fundamental characteristics. Based on this knowledge, full-surface shear stress vector visualization and measurement methodologies were formulated and successfully demonstrated. The present paper reviews the observations and measurements that led to the development of these methodologies and applications are discussed.

List of symbols

C	camera
D	jet exit diameter
GSP	geometric stagnation point
H	hue
H_{VA}	vector-aligned hue, i.e., H at $\phi_C = \phi_\tau$
HSI	hue, saturation, intensity
L	light; or jet tube length
M	Mach number at jet exit centerline or in tunnel freestream
P_∞	ambient pressure
P_o	stagnation pressure at jet exit centerline
Re	freestream unit Reynolds number for tunnel flow; or Reynolds number at jet exit centerline based on D
RGB	red, green, blue
SSLCC	shear-sensitive liquid crystal coating
X	axial coordinate on test surface; origin at jet exit for tangential jet and at disc center for impinging jet
ΔX	spacing between two X locations
Y	transverse coordinate on test surface; zero at X axis
ΔY	spacing between two Y locations
α	above-plane angle, measured positive upward from zero in plane of test surface; or, model angle of attack
β	relative in-plane view angle between shear vector and observer's in-plane line of sight
θ	tilt angle about center of test surface
λ_D	dominant wavelength, inversely proportional to hue
τ	magnitude of surface shear stress vector
τ/τ_r	relative surface shear stress magnitude
ϕ	circumferential angle in plane of test surface, measured positive counter-clockwise from origin on negative X axis
ϕ_τ	orientation of surface shear stress vector directed away from observer with an in-plane line of sight at $\phi = \phi_\tau$

Subscripts

C	camera
J	jet
L	light
P	probe
r	reference value
X	denotes tilt about X axis
Y	denotes tilt about an axis through center of test surface parallel to Y axis

21st ICAS Congress
13-18 September 1998
Melbourne, Australia

Introduction

The objective of this continuing research is to develop an image-based instrumentation system for the areal visualization and measurement of the instantaneous shear stress vector distribution acting on any aerodynamic configuration. In fundamental experiments, continuous full-surface measurements of both the magnitudes and the directions of such skin-friction forces would provide modelers with detailed data sets for code-validation purposes, ultimately leading to more advanced design tools. Further, the application of such a visualization and measurement capability to the testing of advanced aerodynamic configurations would increase both the productivity of wind tunnels and the value of the acquired data sets. The synergistic coupling of surface shear stress patterns with integral force and moment data would allow testers to rapidly and definitively identify cause-and-effect relationships between flowfield and/or configurational variations and resultant aerodynamic consequences.

The approach to accomplish these goals has been to systematically explore the color-change responses of shear-sensitive liquid crystal coatings (SSLCC) to applied shear stresses of known magnitudes and known directions relative to the observer.

Shear-Sensitive Liquid Crystal Coatings

The liquid crystal phase of matter is a weakly ordered, viscous, fluidlike state that exists between the nonuniform liquid phase and the ordered solid phase of certain organic compounds. Liquid crystals can exhibit optical properties that are characteristic of solid, crystalline materials. If a thin film of liquid crystals is applied to a solid surface and the molecules within the coating are aligned by frictional forces into the required planar state, then this molecular arrangement selectively scatters incident white light as a three-dimensional spectrum.

It has been known for some time that changes in applied shear stress magnitude cause the liquid crystal molecular arrangement to change, reorienting the scattered light spectrum in space. A fixed observer thus sees color change in response to the altered shearing force. Such color changes are continuous and reversible, with time response on the order of milliseconds.

Shear Magnitude and Direction Responses

Research conducted at NASA Ames has shown that SSLCC color-change response to shear depends on both shear stress magnitude and the direction of the applied shear vector relative to the observer's in-plane line of sight.[1] Under normal white light illumination and for oblique above-plane observation, color video images of a SSLCC subjected to surface shear stress vectors of known direction showed that any point exposed to a shear vector with a component directed away from the observer exhibited a color-change response. This response was characterized by a shift from the no-shear orange color toward the blue end of the visible spectrum, with the extent of the color change being a function of both shear magnitude and shear direction relative to the observer (Fig. 1a). Conversely, any point exposed to a shear vector with a component directed toward the observer exhibited a non-color-change response, always characterized by a rusty-red or brown color, independent of both shear magnitude and shear direction (Fig. 1b).

These SSLCC color-change responses were quantified by subjecting a planar coating to a wall-jet shear flow; scattered-light spectra were measured at a point on the wall-jet centerline using a fiber-optic probe and a spectrophotometer[1] (Fig. 2). At any fixed shear stress magnitude, the maximum color change was always measured when the shear vector was aligned with and directed away from the observer; changes in the relative in-plane view angle to either side of this vector/observer aligned orientation resulted in symmetric Gaussian reductions in measured color change (Fig. 3). For this vector/observer aligned orientation, color change was found to continually increase with increasing relative shear stress magnitude (Fig. 4). Based on these observations and point-measurement results, full-surface shear stress vector visualization[2] and measurement[3] methodologies were formulated and successfully demonstrated. One example of each application will be reviewed later in this paper.

Surface-Inclination Effects

Experiments have been initiated at NASA Ames to begin the process of quantifying surface-inclination (surface-curvature) effects on the shear vector measurement methodology. The apparatus used for this purpose is shown in Fig. 5.

An axisymmetric, turbulent wall jet of initial diameter 0.33 in. blows tangentially across the test surface, a

smooth, flat, 8 in. diameter disc. Total pressure at the jet exit centerline is monitored and controlled by a feedback loop, as described in Reference 3. Two important new features were added to the apparatus of Reference 3 for these experiments: (1) the jet tube is now locked directly to the circumference of the test plate; (2) the test surface can be systematically tilted about either of two orthogonal axes through its center by the insertion and rotation of interchangeable, inclined-surface, plates (see again Fig. 5). This arrangement ensures that the same shear stress vector distribution is applied to the test surface at all surface-inclination angles.

Surface-inclination angles θ_X, θ_Y of 0, ±5, ±10, and ±15 deg were employed. Since the wall-jet axis is aligned with the X axis, θ_X inclination angles simulate surface slope variations transverse to the principal flow direction (such as would be experienced for flow along a fuselage), while θ_Y inclination angles simulate surface slope variations along the principal flow direction (such as would be encountered for flow over a two-dimensional airfoil).

In this arrangement, white-light illumination was positioned normal to the untilted test surface, and the camera above-plane view angle was set at 30 deg relative to the untilted test surface. A new SSLCC (Hallcrest mixture BCN/192), of nominal thickness 0.002 in., was applied to the test surface for each preset θ_X or θ_Y value. Color (hue) of the coating was then measured with a 3-CCD video camera focused on a small 5x5 pixel area at the center of the test plate for sequentially-applied jet total pressures of 0, 2, and 4 psig (shear magnitudes of 0, 0.27, and 0.53 psf).

Resultant vector-aligned hue measurements "at a point" on the wall-jet centerline are shown in Fig. 6 versus surface-inclination angles θ_X and θ_Y with jet total pressure as the parameter. As can be seen, vector-aligned hue values showed no dependence on θ_X or θ_Y for absolute values of these tilt angles ≤ 15 deg. Acquisition and analyses of full-surface color images are presently underway to more definitively document the insensitivity limits of the shear vector measurement methodology to surface-slope variations.

Qualitative Aspects: Visualization of Transition and Separation

To capitalize on the unique shear-direction-indicating capabilities of SSLCCs, two opposing-view, synchronized, color video cameras need to be deployed: one with an oblique, downstream-facing view of the test surface and the other with an oblique, upstream-facing view. Present understanding dictates that the test surface be planarlike, i.e., no regions of extreme curvature, and that it be uniformly illuminated from above. Figure 7 shows a schematic of the experimental arrangement utilized to demonstrate this new technique.[2]

A generic commercial-transport model with a tip-to-tip wing span of 67 in. was positioned on the centerline of the Boeing 8 x 12 ft. transonic wind tunnel. The model had a cylindrical 8-in. diameter centerbody with boundary-layer trips positioned near the nose; the wings were 12-in. root chord and were swept back at a 35-deg angle. No trips were present on the inboard two-thirds span of the test wing.

The test surface was the upper surface of the starboard wing. The inboard portion of this wing was positioned directly below one of the off-centerline window ports and could thus be uniformly illuminated by a white light (L) from above. Two synchronized, opposing-view color video cameras (C) were deployed. The downstream-facing camera was a miniature device positioned within a vent slot in the tunnel ceiling; this placement yielded an optimum 30-deg above-plane view angle of the wing upper surface at zero degrees angle of attack. The upstream-facing camera was positioned outside the test section, within the surrounding plenum chamber, and viewed the test surface through a window at a 43-deg above-plane viewing angle when the model was at 0-deg angle of attack.

In this arrangement, transition to turbulence on the wing upper surface, characterized by an abrupt increase in surface shear stress magnitude in the principal flow direction, was made visible by the SSLCC color-change response recorded with the downstream-facing camera. Conversely, regions of reverse flow enveloped by upstream-directed shear vectors were made visible by the SSLCC color-change response recorded with the upstream-facing camera. Regions of the coated test surface exposed to shear vectors directed toward either camera yielded no color-change response, appearing as either dark or reddish-brown zones, depending on the absolute light levels reaching the camera. Any regions of extreme transverse flow, enveloped by shear vectors directed either inboard or outboard and approximately perpendicular to the principal flow direction, would have appeared (if present) as a yellow color-change response simultaneously to both cameras.[1]

Figure 8 illustrates the transition-front visualization capability of the SSLCC technique. Here, regions of low shear magnitude were delineated by a red or yellow color, whereas regions of high shear magnitude appeared as green or blue. Several important features of the surface shear field were made visible by these SSLCC color-change responses. Transition at 0-deg angle of attack, for M = 0.4 and Re = 2.5 x 10^6/ft., was seen to occur along a swept line ranging from ~25% of chord inboard to ~75% of chord outboard with turbulent wedges interspersed. This chordwise transition front moved forward with increasing angle of attack consistent with a dependence on the adverse-pressure-gradient onset location for this airfoil section. The discrete turbulent wedges originating from the wing leading-edge region were a result of isolated roughness elements caused by freestream contaminants impacting the surface.

Figure 9a shows synchronized SSLCC color-change responses as recorded by opposing-view cameras for α = 8 deg at M = 0.4 and Re = 2.5 x 10^6/ft. Under these test conditions, a leading-edge separation occurred outboard on the wing upper surface, as indicated by the red zone in the downstream-facing view and the corresponding yellow zone in the upstream-facing view. High-shear (turbulent) attached flow existed everywhere else on the wing upper surface, as indicated by the blue color in the downstream-facing view and no color-change response in the upstream-facing view.

Figure 9b shows synchronized SSLCC color-change responses as recorded by opposing-view cameras for α = 5 deg at M = 0.8 and Re = 3.4 x 10^6/ft. Under these test conditions, a normal shock wave/laminar boundary-layer interaction occurred slightly downstream of the wing leading edge. Here, the yellow zone along the wing leading edge, recorded by the downstream-facing camera, indicated a low-shear (laminar) region upstream of the interaction. A narrow band of reverse flow formed beneath the interaction region, oriented approximately parallel to the leading edge; this region was indicated by the reddish-brown band in the downstream-facing view and, simultaneously, by the yellow band in the upstream-facing view. This reverse-flow region was breached by numerous turbulent wedges seen emanating from aforementioned roughness elements along the leading edge; passage of these locally attached turbulent wedges through the interaction region are best illustrated by the dark breaks in the yellow band recorded by the upstream-facing camera. High-shear (turbulent) attached flow existed everywhere downstream of the reverse-flow region, as indicated by the extensive blue zone in the downstream-facing view, and corroborated by the absence of color change downstream of the yellow band in the upstream-facing view.

Quantitative Aspects: Measurement of Shear Vector Distributions

For full-surface shear stress vector measurements, a 3-CCD RGB video camera, a frame grabber, and a supporting computer are utilized. Figure 10 shows a schematic of the deployment, data acquisition, and data analysis components of this method. The coated surface is illuminated from the normal direction and the camera is positioned at a constant above-plane view angle, α_c ~ 30 deg. Full-surface images of the SSLCC color-change response to an unknown shear field are recorded from multiple in-plane view angles encompassing the shear vector directions to be measured (here, ϕ_{c1} to ϕ_{c4}). For each physical point on the test surface, a Gaussian curve is fit to the hue versus in-plane view angle data. The in-plane view angle corresponding to the maximum of the curve-fit determines the vector orientation (ϕ_τ). The vector-aligned hue value is then converted to a shear magnitude (τ) via a calibration curve acquired using conventional point-measurement techniques (e.g., the fringe-imaging skin friction or "oil-drop" technique of Reference 4).

SSLCC vector measurement resolution and accuracy issues were discussed in detail in References 3 and 5. Uncertainties of 2 to 4% in shear vector magnitude and less than 1 deg in shear vector orientation have been attained. The SSLCC method has been validated against independent oil-drop skin-friction measurements not used in the calibration process.[3],[6]

This methodology was applied to measure the shear stress vector distribution on a planar surface beneath an inclined, axisymmetric, turbulent impinging jet.[6] Figure 11 shows a schematic of this experimental arrangement.

A twenty-frame-average RGB image of the complete test surface was recorded from each of fifteen ϕ_c orientations over the arc $0 \leq \phi_c \leq 180$ deg. Due to the widely varying RGB intensities experienced within each such color image, all ϕ_c images were recorded at two or more exposure settings then mathematically

combined to form a single, composite image wherein each pixel was correctly exposed. All such composite images were low-pass filtered using a 5x5 pixel mask and converted from RGB to an HSI color space.

Taking advantage of the symmetry of the flow field, the time-averaged, filtered hue images for $0 \leq \phi_c \leq 180$ deg were mirror-imaged across the plane of symmetry (the X axis) to form a complete $0 \leq \phi_c \leq 360$ deg image set. These hue images were then subjected to the image processing and data analysis procedure outlined in Fig. 10. The resulting surface shear stress vector distribution is shown in Fig. 12.

This measured data set contains approximately 2×10^5 non-zero vectors, one at every point on a surface grid whose resolution is 100x100 points per square inch. False color levels are used to represent shear stress magnitudes. Black regions represent the absence of a vector value due either to thresholding at the lowest non-zero calibration point or to the failure to attain an acceptable Gaussian curve fit to the H vs. ϕ data set at a particular surface grid point. Vector orientations are illustrated by the vector cross-cut profiles drawn every $\Delta X/D = \pm 1$ starting at the Y axis; for clarity, only every fifth vector, spaced at $\Delta Y/D = 0.15$, is shown in each profile.

A local minimum in shear magnitude was seen to occur in the immediate vicinity of the geometric stagnation point (GSP). Shear magnitude increased rapidly in all directions emanating from the stagnation zone as the inclined-jet flow turned to align itself with the plate surface, then accelerated outwards. Peak shear stresses were measured in all radial directions within 2D of the GSP.

Figure 13 shows the shear magnitude distribution on the X axis, along with the oil-drop data used for calibration purposes. A shear minimum occurred just to the negative X side of the GSP. Due to thresholding applied in the SSLCC method, and/or possibly to unsteadiness observed in this region, a non-zero value of the time-averaged shear magnitude was measured at the stagnation point.

Figure 14 shows continuous measurements from the SSLCC method versus point measurements from the oil-drop method as acquired on a transverse cross-cut at X/D = 2. None of the oil-drop data shown here were used to generate the H_{VA} vs. τ calibration curve. Once again, very good overall agreement was noted between shear vector magnitudes and shear vector orientations measured by these two methodologies. These results provided the first demonstration of the capability of the SSLCC method to reliably measure continuous shear stress vector distributions on planar surfaces where shear vectors of all possible orientations were present.

Summary

The shear-sensitive liquid crystal coating method provides a full-surface diagnostic technique for both the visualization and measurement of continuous shear stress vector distributions.

Acknowledgements

The participation of M.C. Wilder in this research was funded by NASA contract NAS2-14109 to MCAT, Inc., Mountain View, CA.

References

[1] Reda, D.C. and Muratore, J.J., Jr., "Measurement of Surface Shear Stress Vectors Using Liquid Crystal Coatings," *AIAA Journal*, Vol. 32, No. 8, 1994, pp. 1576-1582.

[2] Reda, D.C., Wilder, M.C., and Crowder, J.P., "Simultaneous, Full-Surface Visualizations of Transition and Separation Using Liquid Crystal Coatings", *AIAA Journal*, Vol. 35, No. 4, 1997, pp. 615-616.

[3] Reda, D.C., Wilder, M.C., Farina, D.J., and Zilliac, G., "New Methodology for the Measurement of Surface Shear Stress Vector Distributions," *AIAA Journal*, Vol. 35, No. 4, 1997, pp. 608-614.

[4] Zilliac, G., "Further Developments of the Fringe-Imaging Skin Friction Technique," NASA TM 110425, Dec. 1996.

[5] Wilder, M.C and Reda, D.C., "Uncertainty Analysis of the Liquid Crystal Coating Shear Vector Measurement Technique," AIAA 98-2717, 20th AIAA Advanced Measurement and Ground Testing Technology Conference, Albuquerque, NM, June 15-18, 1998.

[6] Reda, D.C., Wilder, M.C., Mehta, R., and Zilliac, G., "Measurement of the Continuous Pressure and Surface Shear Stress Vector Distributions Beneath an Inclined, Impinging Jet Using Coating and Imaging Techniques," AIAA 97-2489, 32nd Thermophysics Conference, Atlanta, GA, June 23-25, 1997 (accepted for publication, *AIAA Journal*, 1998).

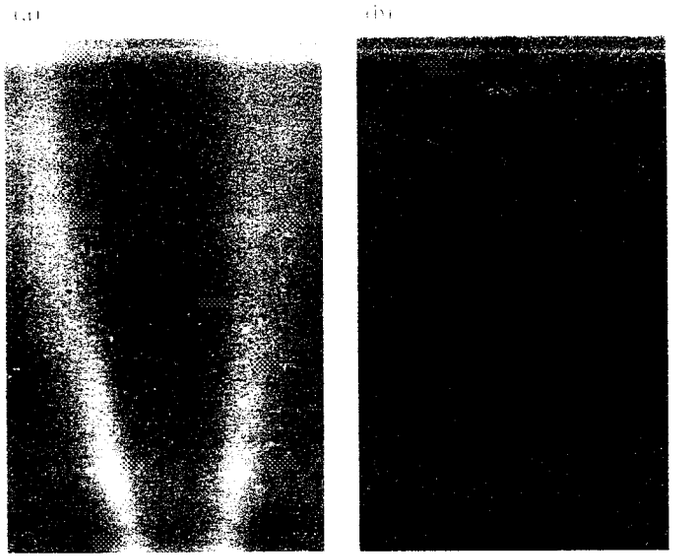

FIGURE 1 - Color-Change Response of Liquid Crystal Coating to Tangential Jet Flow, $\alpha_L = 90°$, $\alpha_C = 35°$: (a) Flow Away From Observer, (b) Flow Toward Observer.

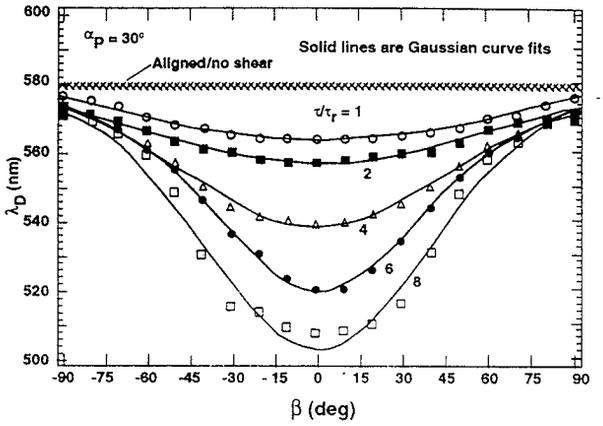

FIGURE 3 - Dominant Wavelength vs. Relative In-Plane View Angle Between Observer and Shear Vector, With Relative Shear Magnitude as the Parameter.

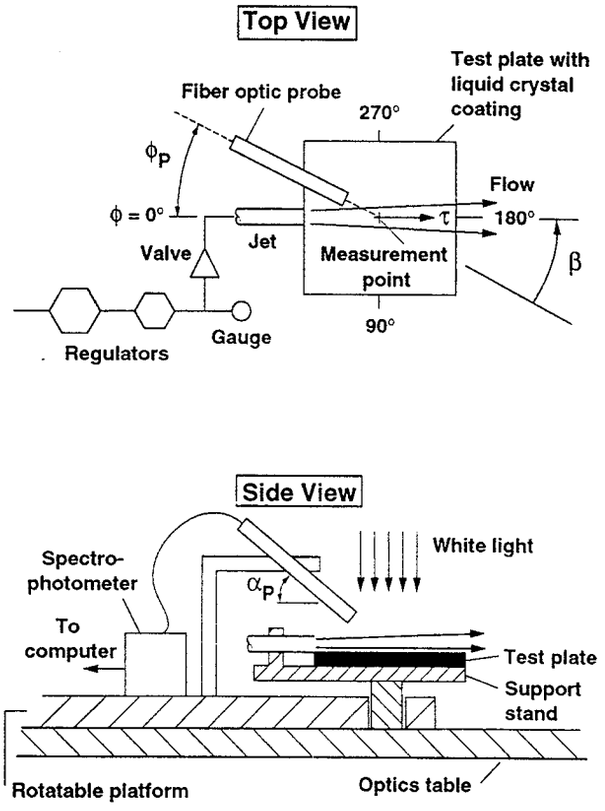

FIGURE 2 - Schematic of Experimental Arrangement for Spectrophotometer Measurements on Centerline of Tangential Jet.

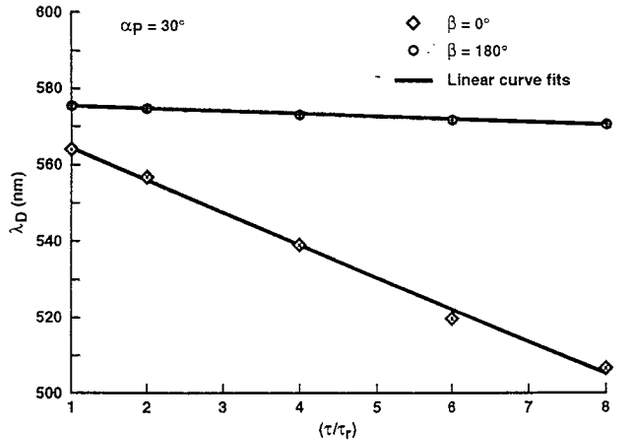

FIGURE 4 - Dominant Wavelength vs. Relative Shear Magnitude for Relative In-Plane View Angles of 0° and 180°.

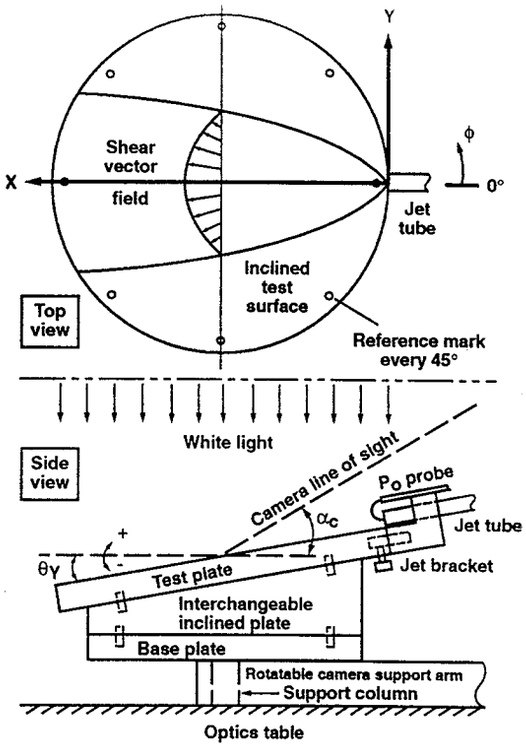

FIGURE 5 - Schematic of Experimental Arrangement for Quantification of Surface-Inclination Effects.

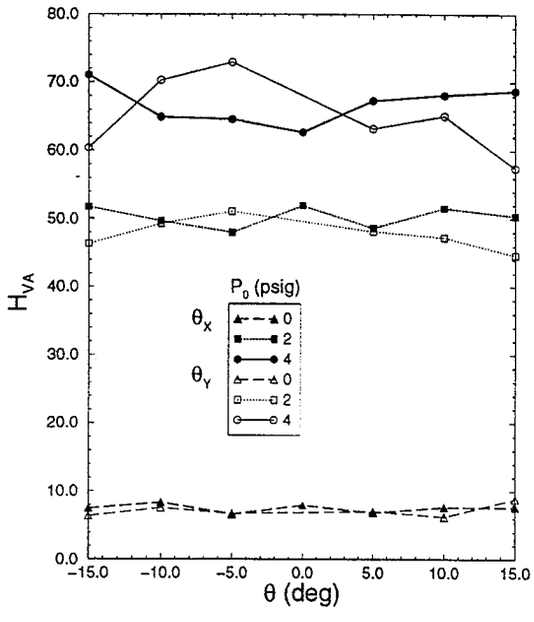

FIGURE 6 - Vector-Aligned Hue at Center of Test Surface vs. Surface-Inclination Angle With Jet Total Pressure as the Parameter.

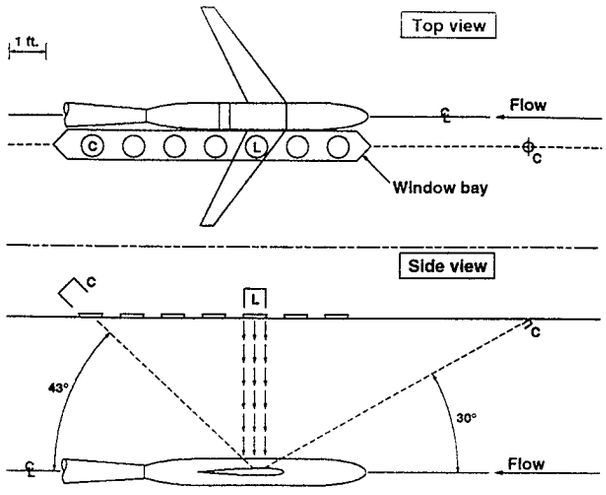

FIGURE 7 - Schematic of Experimental Arrangement for Visualizations of Transition and Separation in Boeing Transonic Wind Tunnel.

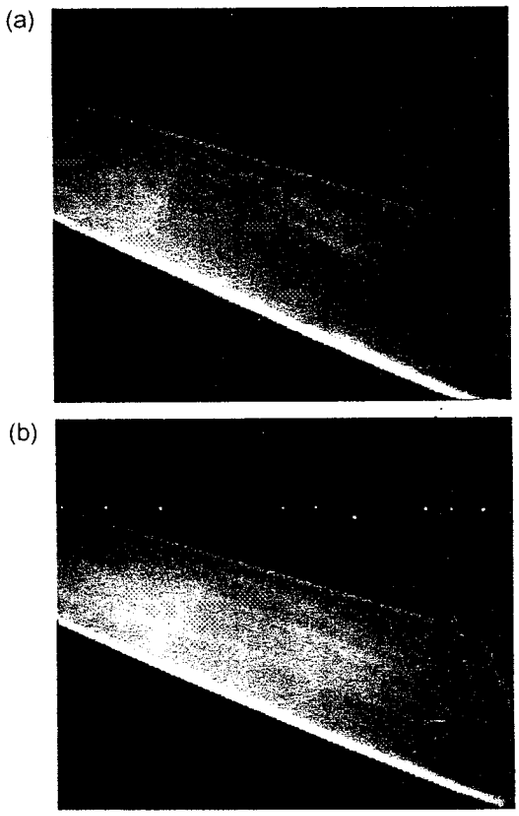

FIGURE 8 - Transition-Front Visualizations Recorded by Downstream-Facing Camera at M = 0.4 and Re = 2.5 x 10^6/ft: (a) $\alpha = 0°$; (b) $\alpha = 2.3°$.

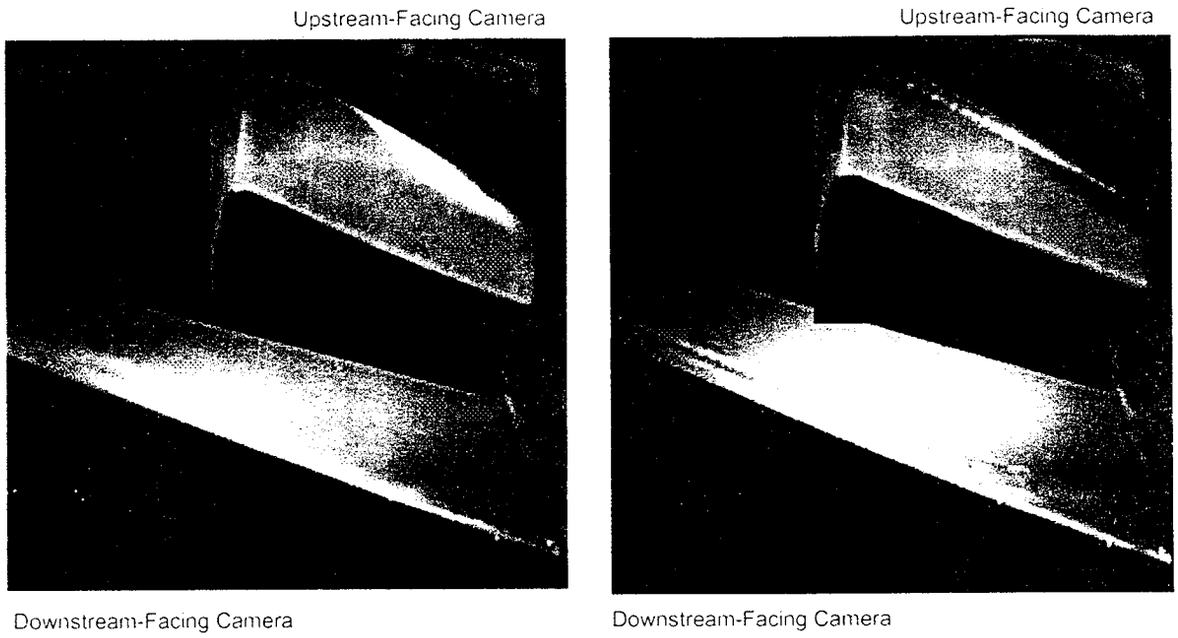

FIGURE 9 - Color-Change Response as Recorded by Opposing-View Cameras: (a) Leading-Edge Separation, $\alpha = 8^{o}$, M = 0.4, Re = 2.5 x 10^{6}/ft; (b) Normal-Shock/Boundary-Layer Interaction, $\alpha = 5^{o}$, M = 0.8, Re = 3.4 x 10^{6}/ft.

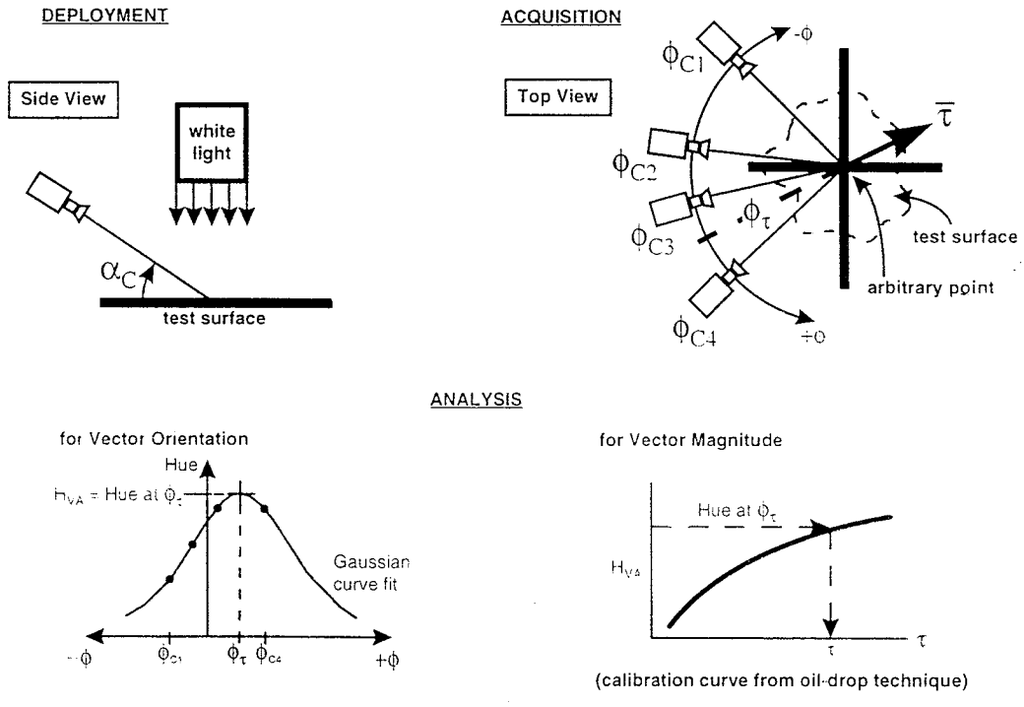

FIGURE 10 - Schematic of Full-Surface Shear Stress Vector Measurement Methodology.

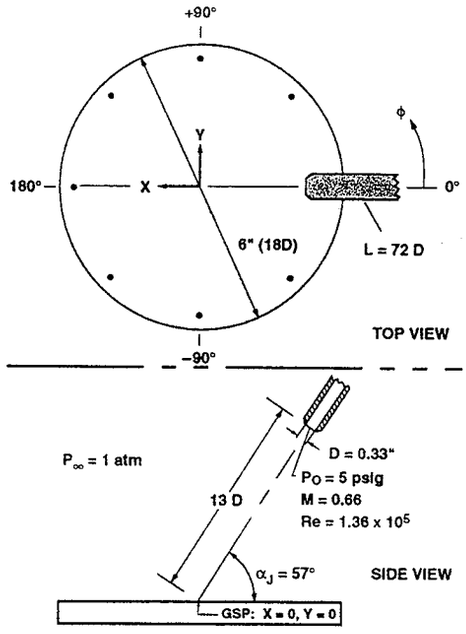

FIGURE 11 - Schematic of Experimental Arrangement for Measurement of Shear Vector Distribution Beneath an Inclined, Impinging Jet.

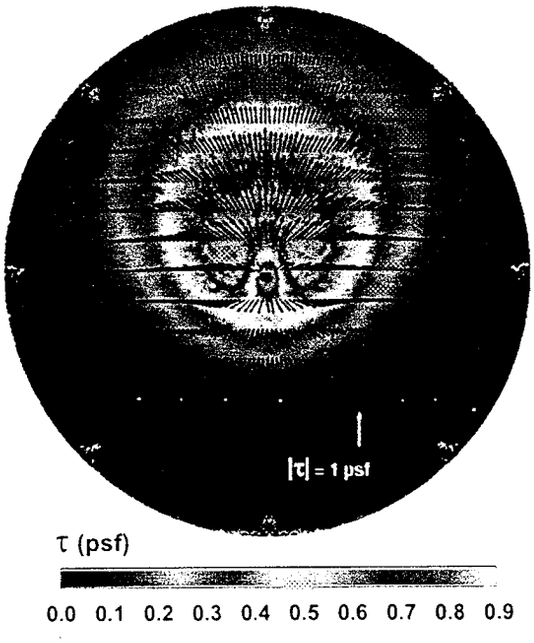

FIGURE 12 - Measured Surface Shear Stress Vector Field Beneath Inclined, Impinging Jet: Color Contours Show Vector Magnitudes and Vector Cross-Cut Profiles Every ΔX/D = 1 Show Vector Orientations.

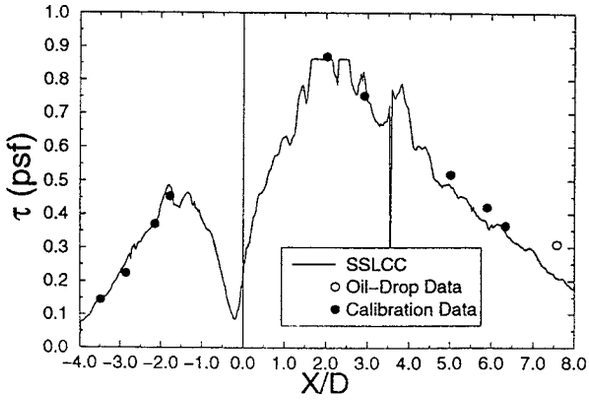

FIGURE 13 - Shear Magnitude Distribution Along X Axis For Inclined, Impinging Jet.

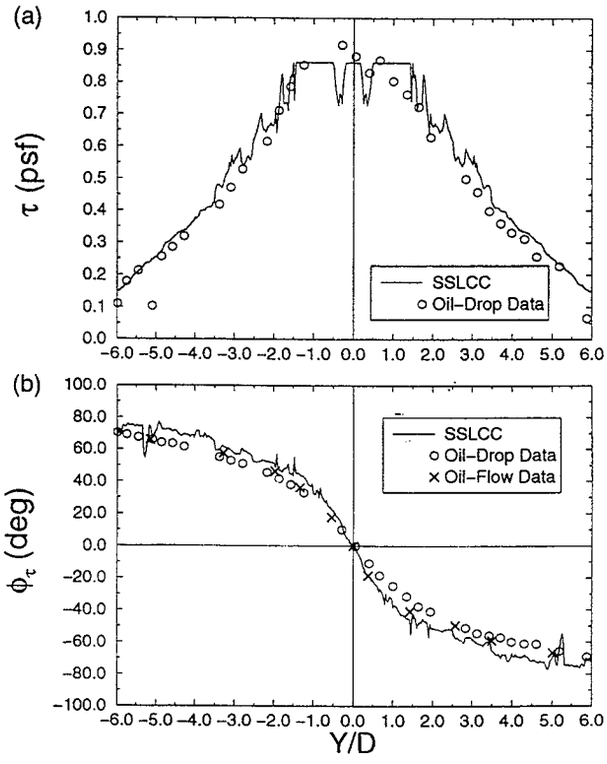

FIGURE 14 - Cross-Stream Profiles of Shear Vector Field Beneath Inclined, Impinging Jet at X/D = 2: (a) Magnitudes vs. Oil-Drop Data; (b) Orientations vs. Oil-Drop and Oil-Flow Data.